Final Draft
of the original manuscript:

Na Ranong, C.; Hoehne, M.; Franzen, J.; Hapke, J.; Fieg, G.; Dornheim, M.; Eigen, M.; Bellosta von Colbe, J.; Metz, O.:

Concept, Design and Manufacture of a Prototype Hydrogen Storage Tank Based on Sodium Alanate

1

Concept, Design and Manufacture of a Prototype Hydrogen Storage Tank Based on Sodium Alanate

Chakkrit Na Ranong*, Merle Höhne, Jens Franzen, Jobst Hapke, Georg Fieg,
Martin Dornheim, Nico Eigen, Jose Maria Bellosta von Colbe, Oliver Metz

Dr.-Ing. Ch. Na Ranong, Dr.-Ing. M. Höhne, J. Franzen,
Prof. Dr.-Ing. J. Hapke, Prof. Dr.-Ing. G. Fieg
Institute of Process and Plant Engineering
Hamburg University of Technology
D-21071 Hamburg
E-mail: c.naranong@tu-harburg.de

Dr. M. Dornheim, Dr.-Ing. N. Eigen,
Dr. J.M. Bellosta von Colbe, O. Metz
Institute of Materials Research
GKSS Research Centre
D-21502 Geesthacht

2

Abstract

In the framework of EC-project STORHY (Hydrogen Storage for Automotive Applications) the prototype of a solid storage tank for hydrogen based on sodium alanate is developed. A storage tank containing 8 kg of sodium alanate is designed and manufactured with the objective of fast refueling. To obtain the optimum design of the storage tank a simulation tool is developed and validated by experiments with a laboratory-scale tubular reactor. Application of the simulation tool to different storage concepts and geometries yields the final design. The chosen concept is modular enabling simple scale-up. This is the basis for the future development of fuel cell vehicle storage tanks containing 5 kg of hydrogen.

1. Introduction

Hydrogen storage is a key enabling technology for the automotive use of hydrogen and for the mass market entry of hydrogen fuelled vehicles [1]. In the framework of EC-project STORHY the potential of different technologies of hydrogen storage for applications in fuel cell vehicles are investigated and evaluated. The automotive industry has formulated requirements for hydrogen storage on-board of a hydrogen-fuelled vehicle [1]. Independent of type of storage 5 kg of hydrogen have to be stored. The resulting driving range will be approximately 400 km. Further requirements are fast refueling and a high volumetric and gravimetric storage density [1]. There are three types of hydrogen storage principles: high pressure storage tanks for gaseous hydrogen, cryogenic storage tanks for liquid hydrogen and solid storage tanks.

The Institute of Process and Plant Engineering conferring with GKSS Research Centre has developed the prototype of a solid storage tank. The storage is based on a reversible chemical reaction between hydrogen and sodium alanate which is a light metal hydride. Metal hydrides in general have the advantage of high volumetric storage density under low operating pressures. Since hydrogen is chemically bonded it can be safely stored for an unlimited period of time with negligible leakage rates [2].

The most important design criterion is fast refueling of the storage tank with hydrogen. This exothermic process requires special care with respect to the thermal design. The stress analysis for the hydride storage tank is determined by the given pressure level of 100 bar. To achieve high storage densities, passive masses due to necessary heat transfer surfaces and pressure retaining vessel walls are minimized. The optimum storage tank design is tailored to the given material applying a simulation tool to different storage tank concepts and geometries. At the Institute of Process and Plant Engineering different metal hydride systems like hydrogen storage tanks, hydrogen compressors, heat storage systems and heat transformers have been modeled and designed by a continuously enhanced simulation tool [3, 4, 5 ,6]. This model-based simulation tool is extended taking into account the special features of sodium alanate which reacts with hydrogen in two steps.

2. Equilibrium and Kinetic Data of Sodium Alanate

Due to the latest developments on the field of light metal hydride sodium alanate has been specified as the active material in this project [1]. This material is especially promising because of its high theoretical hydrogen capacity of 5.6 % and the feasibility of large-scale synthesis [7, 8]. The practical hydrogen capacity strongly depends on the synthesis method of the storage material and the applied catalyst. The effective kinetic is continuously improved

during the project while the practical hydrogen capacity is varying between 3.5 % and 4.85 % [7].

Table 1 shows the characteristics of the reversible chemical reaction between the active material and hydrogen. Starting point is an equimolar mixture of sodium hydride and aluminum. This mixture contains additional catalysts and compounds enhancing the effective thermal diffusivity of the hydride bed [7, 9, 10]. The total reaction consists of two steps, Table 1. In this work the reaction steps are denoted with β and γ, respectively. Considering hydrogen absorption, in the first reaction step β the complete amount of sodium hydride reacts with a portion of the initially provided aluminum and hydrogen to the intermediate product Na_3AlH_6. In the second step γ this intermediate product reacts with further hydrogen and the remaining aluminum to sodium alanate. The absorption reaction of hydrogen is exothermic, the desorption reaction of hydrogen is endothermic. The total enthalpy of reaction is 40 kJ per mole hydrogen.

The equilibrium data of the hydride-hydrogen-system have been determined experimentally [5]. The equilibrium pressure of each reaction step is a function of temperature only, Eqs. (1) and (2).

$$\ln\left(\frac{p_{eq,\beta}}{p_0}\right) = \frac{-49014\,\frac{J}{mol}}{RT} - \frac{-130.21\,\frac{J}{mol\,K}}{R} \tag{1}$$

$$\ln\left(\frac{p_{eq,\gamma}}{p_0}\right) = \frac{-33096\,\frac{J}{mol}}{RT} - \frac{-113.72\,\frac{J}{mol\,K}}{R} \tag{2}$$

The equilibrium data indicate the necessary conditions for hydride formation and decomposition. For hydrogen absorption the loading pressure at the refueling station must be higher than the equilibrium pressure ($p > p_{eq}$). For hydrogen desorption the discharging pressure to the fuel cell must be lower than the equilibrium pressure ($p < p_{eq}$).

Exemplarily, a loading pressure of 100 bar and a discharging pressure of 10 bar are considered. These are typical values for refueling and fuel cell operation, respectively [1]. During exothermic absorption of hydrogen the equilibrium pressure of reaction step β is lower than 100 bar as long as the temperature of the hydride bed is kept below 260 °C, Table 2. The equilibrium pressure of reaction step γ is lower than 100 bar as long as the temperature of the hydride bed is kept below 166 °C, Table 2.

The decomposition of sodium alanate ($NaAlH_4$) starts with reaction step γ. The equilibrium pressure of reaction step γ is higher than 10 bar as long as the temperature of the hydride bed is kept above 77 °C, Table 2. The equilibrium pressure of reaction step β is higher than 10 bar as long as the temperature of the hydride bed is kept above 168 °C, Table 2. For a given operating pressure of the fuel cell of 10 bar the minimum discharging temperature for the endothermic decomposition of Na_3AlH_6 in reaction step β is 168 °C, while the decomposition of sodium alanate ($NaAlH_4$) in reaction step γ requires only a temperature of 77 °C.

The equilibrium data allow the prediction of the general possibility of hydride formation or decomposition. To obtain mass flow rates of hydrogen out of and into the hydride bed, kinetic

data are required. Equations (3-8) represent the experimentally determined effective kinetic data of hydrogen absorption [5]. The correlations reveal that the rate of change of the degree of reaction ($\dot{X}_\beta$, $\dot{X}_\gamma$) is a function of the degree of reaction itself (X_β, X_γ) and the loading pressure p. An important part of the driving force of the chemical reaction is the deviation of the loading pressure p from the equilibrium pressure p_{eq} expressed as a normalized pressure difference in Eqs. (3) and (4) or a pressure ratio in Eqs. (7) and (8).

Rate of change of the degree of reaction of the first reaction step $\dot{X}_\beta$:

$$\dot{X}_{\beta,1} = 28 \cdot 10^{10} \frac{1}{\text{s}} \exp\left(\frac{-117517 \frac{\text{J}}{\text{mol K}}}{RT}\right) (1 - X_\beta)[-\ln(1 - X_\beta)]^{0.286} \left(\frac{p - p_{eq,\beta}}{p_{eq,\beta}}\right) \tag{3}$$

$$\dot{X}_{\beta,2} = 128928 \cdot 10^3 \frac{1}{\text{s}} \exp\left(\frac{-86446 \frac{\text{J}}{\text{mol K}}}{RT}\right) (1 - X_\beta)\left(\frac{p - p_{eq,\beta}}{p}\right) \tag{4}$$

$$\dot{X}_\beta = \min\left[\dot{X}_{\beta,1}; \dot{X}_{\beta,2}\right] \tag{5}$$

Rate of change of the degree of reaction of the second reaction step $\dot{X}_\gamma$:

$$\dot{X}_{\gamma,1} = 0.5166 \frac{1}{\text{s}} \exp\left(\frac{-54660 \frac{\text{J}}{\text{mol K}}}{RT}\right) X_\beta (1 - X_\gamma)[-\ln(1 - X_\gamma)]^{0.286} \ln\left(\frac{p}{p_{eq,\gamma}}\right)\left(\frac{p}{p_0}\right)^{2.7} \tag{6}$$

$$\dot{X}_{\gamma,2} = 1874.7 \frac{1}{\text{s}} \exp\left(\frac{-62933 \frac{\text{J}}{\text{mol K}}}{RT}\right) X_\beta (1 - X_\gamma)\ln\left(\frac{p}{p_{eq,\gamma}}\right)\left(\frac{p}{p_0}\right)^{1.5} \tag{7}$$

$$\dot{X}_\gamma = \min\left[\dot{X}_{\gamma,1}; \dot{X}_{\gamma,2}\right] \tag{8}$$

3. Metal Hydride Storage Tanks

In the 1980s metal hydride storage tanks for automotive applications have been comprehensively tested in a fleet program [11]. The active material is CODE 5800 ($Ti_{0.98}Zr_{0.02}V_{0.45}Fe_{0.1}Cr_{0.05}Mn_{1.5}$). The practical hydrogen capacity of CODE 5800 is 1.8 %. Material selection has been carefully adjusted to the operating conditions of the internal combustion engine. With respect to some design details these storage tanks are still state-of-the-art. They have been chosen as reference for STORHY [1].

In the frame of the DOE Hydrogen Program Lasher et al. [12] have developed a conceptual design of a sodium alanate tank for 5.6 kg of hydrogen. Ahluwalia [13, 14] has theoretically studied this conceptual design with respect to fuel cell vehicle applications. In the

mathematical model each component of the storage tank is described by a lumped-parameter approach applying mass and energy balance equations. The resulting governing equations are a system of ordinary differential equations, i.e. the spatial distribution of temperatures and hydrogen concentrations are not included.

Also in the frame of the DOE Hydrogen Program Mosher et al. [15, 16] have manufactured and tested two prototypes of sodium alanate based storage tanks. The first prototype contains 19 kg of active material. It served as a demonstrator to identify the key technical challenges like scaled-up material catalysis and processing and powder loading and densification compatible with prototype fabrication. The optimized second prototype is designed at nominal 1/8th scale of the first one to reduce the level of resources needed. The 2007 target of the DOE Hydrogen Program of the system fill time is 10 minutes. The system fill time of the optimized second prototype is 60 minutes [16].

3.1 Working Principle

Figure 1 shows the working principle of a hydride storage tank exemplarily for a tubular reactor. It consists of three components:

1. reactor shell tube,
2. hydride bed and
3. porous sintered metal tube.

During loading hydrogen supplied by the refueling station flows through the sintered metal tube into the hydride bed. The sintered metal tube is permeable for hydrogen but not for the hydride material. It fulfills the function of hydrogen distribution inside the reactor and it works as a filter preventing emission of hydride material out of the storage tank into the surroundings. The hydride bed absorbs hydrogen in an exothermic chemical reaction. The released energy is transferred through the reactor shell tube to the heat transfer fluid. The reactor shell tube separates hydride bed and heat transfer fluid. For operation of a fuel cell, the fully loaded tubular reactor is heated by the heat transfer fluid. In the hydride bed the endothermic desorption reaction takes place. The released hydrogen flows from the hydride bed through the porous sintered metal tube to the fuel cell.

3.2 Design Principles

Figure 2 gives an overview of design solutions for the different components of metal hydride storage tanks. The selection of the final solution is amongst others determined by factors like stage of development of the hydride material, risk of failure during the manufacturing stage, existing and approved designs and available manufacturing technologies.

At the actual stage of material development the focus is on improvement of reaction kinetics while production of formed bodies and compacts (Figure 2) are future projects. Therefore, the packing arrangement of the hydride material is unstructured. The degree of volume expansion of the actual hydride material during operation is currently under investigation. Void volume is included in the design to allow for free expansion of the hydride bed. To avoid inhomogeneities of the porosity of the hydride because of gravity effects the storage tank is positioned horizontally (Figure 2). Because of the loading pressure of 100 bar the packing arrangement is cylindrical (Figure 2). This yields reasonable wall thicknesses of the reactor shell around the hydride material.

Lasher et al. [12] and Mosher et al. [15, 16] have chosen internal heat transfer (Figure2) to the heat transfer fluid. The storage tank design [12, 15, 16] is a single large pressure vessel containing the whole amount of active material. A tube bundle for the heat transfer fluid and a bundle of sintered metal tubes for hydrogen supply are surrounded by the active material (Figure 2, design A).

In STORHY a modular concept is selected to minimize the risk of failure during the manufacturing stage because of the narrow time schedule of the project. If a failure occurs only the defective module of the storage tank has to be replaced. This concept is realized by external heat transfer from a bare tube (Figure 2, design B) to the heat transfer fluid. The total amount of active material is distributed to a number of tubular reactor elements.

Although not manufactured, a new concept for a large hydride vessel with internal cooling has been developed in this work. The simulated performance is discussed in section 4.3. In contrast to Lasher et al. [12] and Mosher et al. [15, 16] hydrogen supply is peripheral (Figure 2) and the heat transfer fluid flows through coiled tubes (Figure 2, design C). Both measures simplify the manifolds of hydrogen and heat transfer fluid (Figure 3).

The favored concept for manufacture is a tube-bundle of reactor elements, which are connected in parallel on the hydrogen side. Depending on the number of required reactor elements different solutions on the heat transfer fluid side are possible following the design of multitube and shell-and-tube heat exchangers, Figure 3.

4. Design Procedure

The hydrogen content w is commonly used to describe refueling processes of hydride materials. This time-dependent quantity is the ratio between absorbed mass of hydrogen to the initial mass of active material, Eq. (9).

$$w = \frac{m_{H_2}}{m_{Me}^0} = \frac{m_{H_2}}{m_{NaH}^0 + m_{Al}^0} \tag{9}$$

The maximum hydrogen content depends on the hydride material, its manufacturing process and kind and amount of additional compounds.

$$w_{max} = \frac{m_{H_2}^{max}}{m_{Me}^0} = \frac{m_{H_2}^{max}}{m_{NaH}^0 + m_{Al}^0} \tag{10}$$

The criterion of fast filling is formulated applying the normalized hydrogen content X. This is the ratio of actual hydrogen content w to the maximum hydrogen content w_{max}. Equation (11) clarifies that the normalized hydrogen content is the ratio of actually absorbed mass of hydrogen to the maximally absorbable mass of hydrogen.

$$X = \frac{w}{w_{max}} = \frac{m_{H_2}}{m_{Me}^0} \frac{m_{Me}^0}{m_{H_2}^{max}} = \frac{m_{H_2}}{m_{H_2}^{max}} \tag{11}$$

The criterion of fast refueling is fulfilled if the storage tank is loaded to 80 % after 600 s and nearly to 100 % after 1000 s, Table 3.

4.1 Modeling and Simulation

To design a storage tank fulfilling the criteria of Table 3 a design tool is required, which is able to pre-calculate the absorbed mass of hydrogen as a function of time for arbitrary storage concepts and geometries. This is achieved by modeling and simulation. Each component of the storage tank is described by balance equations for mass and energy. Exemplarily the balance equations are given for the components of a tubular reactor (Figure 1). The components of other storage concepts like the large hydride vessel (Figure 3) are correspondingly formulated.

A tubular reactor (Figure1) consists of three components: sintered metal tube, hydride bed and reactor shell tube. Hydride bed and the sintered metal tube are porous media [17]. Porous medium "sintered metal tube" (*t*) consists of solid material (*St*) and fluid material (*f*). Solid material of the sintered metal tube is steel 1.4404. The fluid material is pure gaseous hydrogen.

Mass balance equation of the sintered metal tube (Figure1):

$$\varepsilon_t \frac{\partial \rho_f}{\partial t} + \nabla \cdot \left(\rho_f \vec{v}_{f,t} \right) = 0 \tag{12}$$

Darcy's Law for the flow velocity vector in Eqs. (12) and (14):

$$\vec{v}_{f,t} = -\frac{\kappa_t}{\eta_f} \nabla p_t \tag{13}$$

Energy equation of the sintered metal tube:

$$\left[(1 - \varepsilon_t) \cdot (\rho c_p)_{St} + \varepsilon_t (\rho c_p)_f \right] \frac{\partial T_t}{\partial t} + (\rho c_p)_f \vec{v}_{f,t} \nabla T_t = \nabla \cdot \left(k_{eff,t} \nabla T_t \right) \tag{14}$$

Porous medium "hydride bed" (*b*) consists of solid material (*s*) and fluid material (*f*). Solid material is a mixture of NaH, Al, Na_3AlH_6, $NaAlH_4$ and catalysts. Source terms in Eqs. (15) and (17) are describing the chemical reaction.

Mass balance equation of the hydride bed (Figure 1):

$$\varepsilon_b \frac{\partial \rho_f}{\partial t} + \nabla \cdot \left(\rho_f \vec{v}_{f,b} \right) = \rho_s (1 - \varepsilon_b) \left[w_\beta^{max} \dot{X}_\beta + w_\gamma^{max} \dot{X}_\gamma \right] \tag{15}$$

Darcy's Law for the flow velocity vector in Eqs. (15) and (17):

$$\vec{v}_{f,b} = -\frac{\kappa_b}{\eta_f} \nabla p_b \tag{16}$$

Energy equation of the hydride bed:

$$\left[(1-\varepsilon_b)(\rho c_p)_s + \varepsilon_b(\rho c_p)_f\right]\frac{\partial T_b}{\partial t} + (\rho c_p)_f \vec{v}_{f,b}\nabla T_b =$$

$$\nabla\cdot\left(k_{eff,b}\nabla T_b\right) + \rho_s(1-\varepsilon_b)\frac{1}{M_{H_2}}\left[w_\beta^{max}\dot{X}_\beta \Delta H_R^\beta + w_\gamma^{max}\dot{X}_\gamma \Delta H_R^\gamma\right] \tag{17}$$

Energy equation of the reactor shell tube (Figure1):

$$(\rho c_p)_W \frac{\partial T_W}{\partial t} = \nabla\cdot\left(k_W \nabla T_W\right) \tag{18}$$

In the mathematical model heat transfer to the heat transfer fluid appears in the boundary condition of the energy equation (18) of the reactor shell tube at the outer wall surface, Eq. (19). Correlations of heat transfer coefficients h are given in [18] and [19].

$$\vec{n}\left(k_W \nabla T_W\right) = h\left(T_{HF} - T_W\right) \tag{19}$$

The complete set of boundary, coupling and initial conditions of the model are given in [5] and [20]. The model is implemented into the software package COMSOL. The coupled partial differential equations are solved numerically with the finite element method [21]. As result, for each point in time and space the following quantities are known: hydrogen content, temperature, pressure, flow velocity of hydrogen and the degrees of reaction of both reaction steps.

The energy released in the hydride bed during hydrogen absorption is crucial for the thermal design because it has to be removed. The released energy is described by the source terms of Eq. (17). Equation 17 reveals that the released energy depends on the maximum hydrogen contents w_β^{max} and w_γ^{max}. Therefore, the largest observed practical maximum hydrogen content of 4.85 % [7] has been selected for the prototype design, Table 1.

4.2 Validation of the Model

In order to validate the above described model a laboratory-scale tubular reactor was built and technologically tested in charging and discharging experiments (Figure 4). The reactor is filled with 30 g of active material. The active material has to be filled into the reactor under inert glove box conditions due to the reactivity of the hydride material with oxygen and water vapor of the ambient air [1].

The experimental set-up consists of the reactor connected to a hydrogen reservoir by a valve. At the beginning of the experiment the reactor contains no hydrogen and the valve is closed. The reservoir is filled with pressurized hydrogen. A heat transfer fluid is circulated around the reactor. If the valve is opened hydrogen flows from the reservoir into the reactor and the active material absorbs the hydrogen in an exothermic chemical reaction. The quantity of absorbed hydrogen is determined from a mass balance of the gaseous phase of the system whereby the system volume is exactly known. Pressures and temperatures are registered to evaluate the thermal equation of state of hydrogen. Figure 5 shows the results of the experiments for different loading pressures and temperatures of the heat transfer fluid. There is reasonable agreement between experiment and simulation to justify modeling and simulation as an appropriate design tool for hydride storage tanks.

The bottom part of Figure 4 shows the arrangement of seven laboratory scale reactors to a tube bundle demonstrating the feasibility of the modular concept from the manufacturing point of view.

4.3 Simulation Results

The favored concept for manufacture is a tube-bundle of reactor elements, which are connected in parallel on the hydrogen side, see section 3.2. The optimum geometry of a tubular reactor element is found by simulation for the following given operating conditions:

- The initial temperature of the empty system is 80 °C.
- The inlet temperature of the heat transfer fluid (Marlotherm X) is 100 °C.
- The volumetric flow rate of the heat transfer fluid is 12 m^3/h.
- A constant loading pressure of hydrogen of 100 bar is applied.

The wall thickness of the reactor element shell tubes is a function of their outer diameter, given by strength of material calculation. A limiting design factor is the availability of sintered metal tubes. They are only available with an outer diameter of 6 mm.

Figure 6 shows the simulation results for storage tanks with an outer diameter of the reactor elements of 16 mm and 60 mm, respectively. The storage tank with 16 mm reactor elements can be refueled to 80 % in only 290 s, the storage tank with 60 mm reactor elements within 540 s. Both geometries fulfill the criterion of fast refueling. The refueling time of the storage tank with 60 mm reactor elements lies at the upper acceptable limit, Table 3. Therefore the criterion of minimization of passive masses is decisive. As shown in Table 4 the storage tank with 60 mm reactor elements clearly is the optimum solution. The mass of all reactor element shell tubes is only 38 kg compared to 68 kg, and the mass of all sintered metal tubes is only 0.9 kg compared to 17 kg, Table 4. The prototype storage tank will consist of seven 60 mm reactor elements.

The available volumetric flow rate of the heat transfer fluid is 12 m^3/h. It has been taken into account that each reactor element geometry requires its own design on the heat transfer fluid side (Table 4, Figure 3 and Figure 6). For the 16 mm reactor elements a multitube design (Figure 3) allows heat transfer fluid flow over 266 reactor elements with a heat transfer coefficient of 610 W/(m^2 K). For the 60 mm reactor elements only a single tube bundle is necessary (Figure 7). The heat transfer coefficient of this shell-and-tube apparatus is 319 W/(m^2 K).

Although the large hydride vessel with internal heat transfer has not been favored for the manufactured design (section 3.2) its refueling performance is given in Figure 6 to illustrate the performance of an alternative concept. The large hydride vessel is filled to 80 % after 458 s. The predicted refueling period is 82 s shorter than for the shell-and-tube design with 60 mm reactor elements.

5. Manufactured Prototype

Figure 7 shows the prototype. The design is certified according to EC pressure equipment directive 97/23/EC. The conformity assessment procedure of category IV, module G (EC unit verification) has been applied [22]. The calculation code is AD 2000 (calculation pressure: 150 bar, calculation temperature: 300 °C) [23]. All pressure parts are manufactured from the material 1.4571. This austenitic steel is high-pressure hydrogen resistant.

The final prototype is a longitudinal flow shell-and-tube apparatus, Figure 7. The tube bundle consists of seven reactor elements. The sectional view in Figure 7 shows three of seven reactor elements. The heat transfer fluid has one pass on the shell side. During loading hydrogen enters the storage tank through the valve (1). The spiral manifold (2) supplies the hydrogen to the reactor elements (3) which are connected in parallel. The heat transfer fluid enters the storage tank through the inlet nozzle (4) of the shell (5). It flows longitudinally over the reactor elements (3) and leaves through the outlet nozzle (6). The heat transfer fluid is Marlotherm X [24] for safety reasons. In contrast to water it does not chemically react with the active material [1].

The following aspects have been taken into account with special care:

- filling of hydride material into the reactor elements under glove box conditions
- feasibility of assembly of the storage tank components, especially under glove box conditions
- minimization of the number of welding seams, i.e. minimization of leakage risks
- reliable and safe handling during experimental operation
- available production facilities and manufacturing technology
- usage of standardized semi-finished products to accelerate manufacture
- measures in case of repair

The hydrogen manifold (2) lies completely outside of the heat transfer fluid with the advantage that all tube fittings are always accessible during operation, i.e. they can be inspected and refastened. The heat transfer fluid shell (5) is a removable unit. Hydrogen side and heat transfer fluid side can be separately handled.

Figure 8 shows a reactor element. The gastight hydrogen supply tube (10) is fed through the torispherical head (15) and joined by welding to the porous sintered metal tube (7) inside the reactor element. Each reactor element undergoes its own proof test before filling the hydride material. To fill the reactor element with hydride material it is positioned vertically inside a glove box. The hydride material is poured into the reactor through the 8 mm opening (12). After filling, the reactor element is sealed by the closure plug (11). This special design enables proof test before filling and reliable sealing under glove box conditions. At the opposite end the reactor element is fed through flange (13) from the side of the heat transfer fluid to the surroundings.

Figure 9 shows the manufactured prototype. Seven reactor elements which will be connected by the spiral manifold and the filling ends of the reactor elements can be identified.

6. Up-scaling

The chosen concept is modular. The prototype with 8 kg of active material can be scaled up to even larger storage tanks to absorb the amount of hydrogen required by the automotive industry of 5 kg. In this case 82 reactor elements containing approximately 100 kg of active material are required. They can be arranged in accordance with available space in the vehicle. The modular concept has a high degree of formability [1]. While the hydrogen supply spiral (Position (2) in Figure 7) is appropriate for a small number of reactor elements a more advanced hydrogen manifold is necessary for the up-scaled tank with 82 reactor elements. For effective space-usage flat ends of the manifold chamber are preferred to domed ends although this is disadvantageous from the strength of material perspective. To overcome this

disadvantage the thickness of the walls of the manifold chamber with flat ends is significantly reduced by applying stay bolts, Figure 10. Flow channels for hydrogen are drilled into the stay bolts. The stay bolts have two combined functions, providing mechanical stability and distributing hydrogen to the reactor elements.

7. Conclusions and Summary

- A mathematical model as a tool for the thermal design of hydride storage tanks has been developed.
- Necessary correlations of the effective kinetic of the absorption reaction of hydrogen have been experimentally determined.
- The model has been validated by experiments with a laboratory-scale reactor
- The model-based simulation tool has been applied to different storage concepts and geometries.
- Strength of material calculation, manufacturing technology and further requirements like assembly and filling of hydride material under glove box conditions, hydrogen supply and flow configuration of the heat transfer fluid yield the final design of the prototype tank.
- The task to manufacture the prototype of a hydrogen storage tank containing 8 kg of active material has been solved.
- The modular concept enables scale-up to a storage tank with 5 kg of hydrogen.

Table 1: Characteristics of sodium alanate: total reaction and reaction steps

	chemical reaction equation	enthalpy of reaction [kJ/(mol H$_2$)]	hydrogen content [%]
total reaction	3 NaH + 3 Al + 9/2 H$_2$ ⇌ 3 NaAlH$_4$	40	4.85
reaction step β	3 NaH + Al + 3/2 H$_2$ ⇌ Na$_3$AlH$_6$	49	1.85
reaction step γ	Na$_3$AlH$_6$ + 2 Al +3 H$_2$ ⇌ 3 NaAlH$_4$	33	3.00

Table 2: Relevant equilibrium data calculated from Eqs. (1-2). Typical refueling pressure is 100 bar, typical fuel cell pressure is 10 bar.

T [K]	ϑ [°C]	$p_{eq,\beta}$ [bar]	$p_{eq,\gamma}$ [bar]
293	20	0.0117	1.10
350	77	0.306	**10.0**
373	100	0.872	20.3
439	166	9.25	**100**
441	168	**10.0**	105
453	180	14.2	133
533	260	**100**	498

Table 3: Criterion of fast refueling in EC-project STORHY

	t [s]	X [-]
first sub-criterion	600	0.80
second sub-criterion	1000	0.98

Table 4: Comparison between 16 mm and 60 mm reactor elements

outer diameter	[mm]	16	60
length of reactor element	[m]	0.5	1
number of reactor elements for 8 kg of active material	[-]	266	7
mass of all reactor element shell tubes	[kg]	68	38
mass of all sintered metal tubes	[kg]	17	0.9
type of apparatus		multitube	longitudinal flow shell-and-tube
number of tube bundles	[-]	38	1
number of reactor elements per tube bundle	[-]	7	7
outer tube limit (OTL)	[mm]	100	211
flow cross-section of heat transfer fluid	[cm^2]	66	152
wetted perimeter	[m]	0.67	1.98
hydraulic diameter	[mm]	39	31
flow velocity of heat transfer fluid	[m/s]	0.51	0.22
Reynolds number	[-]	41550	14013
Nußelt number	[-]	216	90
heat transfer coefficient	[W/(m^2 K)]	610	319

13

Symbols used

c_p	[J/(kg K)]	specific isobaric heat capacity
ΔH_R	[J/mol]	enthalpy of reaction
h	[W/(m^2 K)]	heat transfer coefficient
k	[W/(m K)]	heat conductivity of solids
k_{eff}	[W/(m K)]	effective heat conductivity of porous medium
M_{H_2}	[kg/mol]	molecular mass of hydrogen
$\vec{n}$	[-]	normal vector
p	[bar]	pressure
p_0	[bar]	reference pressure, $p_0 = 1$ bar
T	[K]	temperature
t	[s]	time coordinate
$\vec{v}_f$	[m/s]	flow velocity vector of hydrogen
w	[-]	hydrogen content
X	[-]	normalized hydrogen content, also degree of the total reaction
X_β	[-]	degree of reaction of step β
X_γ	[-]	degree of reaction of step γ

Greek letters

ε	[-]	porosity
η	[kg/(m s)]	dynamic viscosity
κ	[m^2]	permeability
ρ	[kg/m^3]	density
ϑ	[°C]	temperature

Super- and subscripts
b	hydride bed
f	fluid
HF	heat transfer fluid Marlotherm X
max	maximum
St	solid material of porous sintered metal tube
s	solid material of porous hydride bed
t	sintered metal tube
W	reactor shell tube
β	reaction step
γ	reaction step
0	initial

Accent
.	rate of change

Abbreviations
DOE	United States Department of Energy
STORHY	Hydrogen Storage for Automotive Applications

14

References

[1] www.storhy.net

[2] A. Züttel, in *Hydrogen as a Future Energy Carrier* (Eds.: A. Züttel, A. Borgschulte and L. Schlapbach), Wiley-VCH, Weinheim **2008**

[3] F. Röhl, *Entwicklung, experimentelle Erprobung und Simulation thermochemischer Wasserstoffkompressoren auf der Basis von Metallhydriden*, VDI Fortschrittsberichte, 3 (707)*, VDI Verlag, Düsseldorf **2001**.

[4] M. Höhne, *Simulation und Optimierung eines thermischen Energiespeichers auf Metallhydridbasis*, VDI-Fortschrittsberichte, 3 (812), VDI-Verlag, Düsseldorf **2004.**

[5] J. Franzen, Modellierung und Simulation eines Wasserstoffspeichers auf der Basis von Natriumalanat, *Dissertation*, TU Hamburg-Harburg **2009.**

[6] Ch. Na Ranong et al., Experimental and Theoretical Investigations of a Fuel Cell-Metal Hydride Storage-System, in *Proc. of the 4th Int. Conf. on Heat Transfer, Fluid Mechanics and Thermodynamics* (Eds: J.P. Meyer, A.G. Malan), **2005**.

[7] N. Eigen et al., *Journal of Alloys and Compounds* **2008**, *465 (1-2)*, 310-316. DOI: 10.1016/j.jallcom.2007.10.079

[8] N. Eigen et al., *Scripta Materialia* **2007**, *56 (10)*, 847-851. DOI:10.1016/j.scriptamat.2007.01.024

[9] M. Fichtner et al., *Materials Science and Engineering B* **2004**, *108 (1-2)*, 42-47. DOI: 10.1016/j.mseb.2003.10.036

[10] B. Bogdanovic et al., *Advanced Materials* **2003**, *15 (12)*, 2012-2015. DOI: 10.1002/adma.200304711

[11] Alternative Energie für den Straßenverkehr, Wasserstoffantrieb in der Erprobung, Ed.: Projektbegleitung Kraftfahrzeuge und Straßenverkehr, TÜV Rheinland e.V. im Auftrag des Bundesministers für Forschung und Technologie, Verlag TÜV Rheinland 1989

[12] S. Lasher, E. Carlson, J. Bowman, M. Marion, Y. Yang, Analyses of Hydrogen Storage Materials and On-Board Systems, Annual Progress Report 2005 VI.F.2, DOE Hydrogen Program, **2005**

[13] R.K. Ahluwalia, *Int. J. of Hydrogen Energy* **2006**, *32*, 1251-1261. DOI: 10.1016/j.ifhydene.2006.07.027

[14] R.K. Ahluwalia, J.C. Peng, R. Kumar, System-Level Analysis of Hydrogen Storage Options, Annual Progress Report 2005 VI.F.3, DOE Hydrogen Program, **2005**

[15] D.A. Mosher, X. Tang and S. Arsenault, High Density Hydrogen Storage System Demonstration Using NaAlH4 Based Complex Coumpound Hydrides, Annual Progress Report 2006 IV.A.1, DOE Hydrogen Program, **2006**

[16] D.A. Mosher, S. Arsenault, X. Tang and B.L. Laube, High Density Hydrogen Storage System Demonstration Using NaAlH4 Based Complex Coumpound Hydrides, Annual Progress Report 2007 IV.A.3, DOE Hydrogen Program, **2007**

[17] D. A. Nield, A. Bejan, *Convection in Porous Media*, 2nd ed., Springer-Verlag, New York **1999.**

[18] *VDI Wärmeatlas* (Ed.: Verein deutscher Ingenieure), 10. Auflage, VDI Verlag, Düsseldorf **2006.**

[19] S. Schneider, *Untersuchungen zum lokalen Wärmeübergangsverhalten im Längsstrom-Rohrbündelwärmeübertrager mit geschlitzten Stützblechen*, VDI-Fortschrittsberichte, 19 (106), VDI-Verlag, Düsseldorf **1997.**

[20] O. Ourak, Berechnung des Betriebsverhaltens eines Metallhydridspeichers für Wasserstoff auf Natriumalanatbasis, *Diplomarbeit,* TU Hamburg-Harburg **2008**.

[21] *Comsol Multiphysics Version 3.4.*, Computer Software, COMSOL AB, Copyright **1994-2007.**

[22] *Directive 97/23/EC* of the European Parliament and of the Council of 29 May 1997 on the Approximation of the Laws of the Member States Concerning Pressure Equipment

[23] AD 2000 Code for Pressure Vessels, German Pressure Vessel Association, Beuth, Berlin **2008**

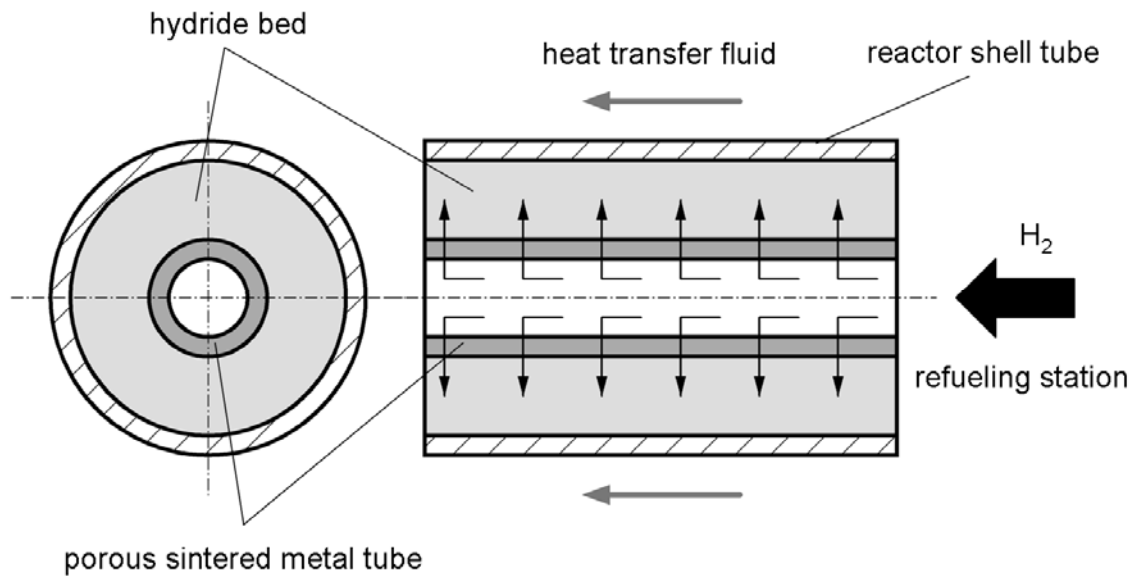[24] W. Wagner, *Wärmeträgertechnik*, 7. Aufl., Vogel Buchverlag, Würzburg **2005.**

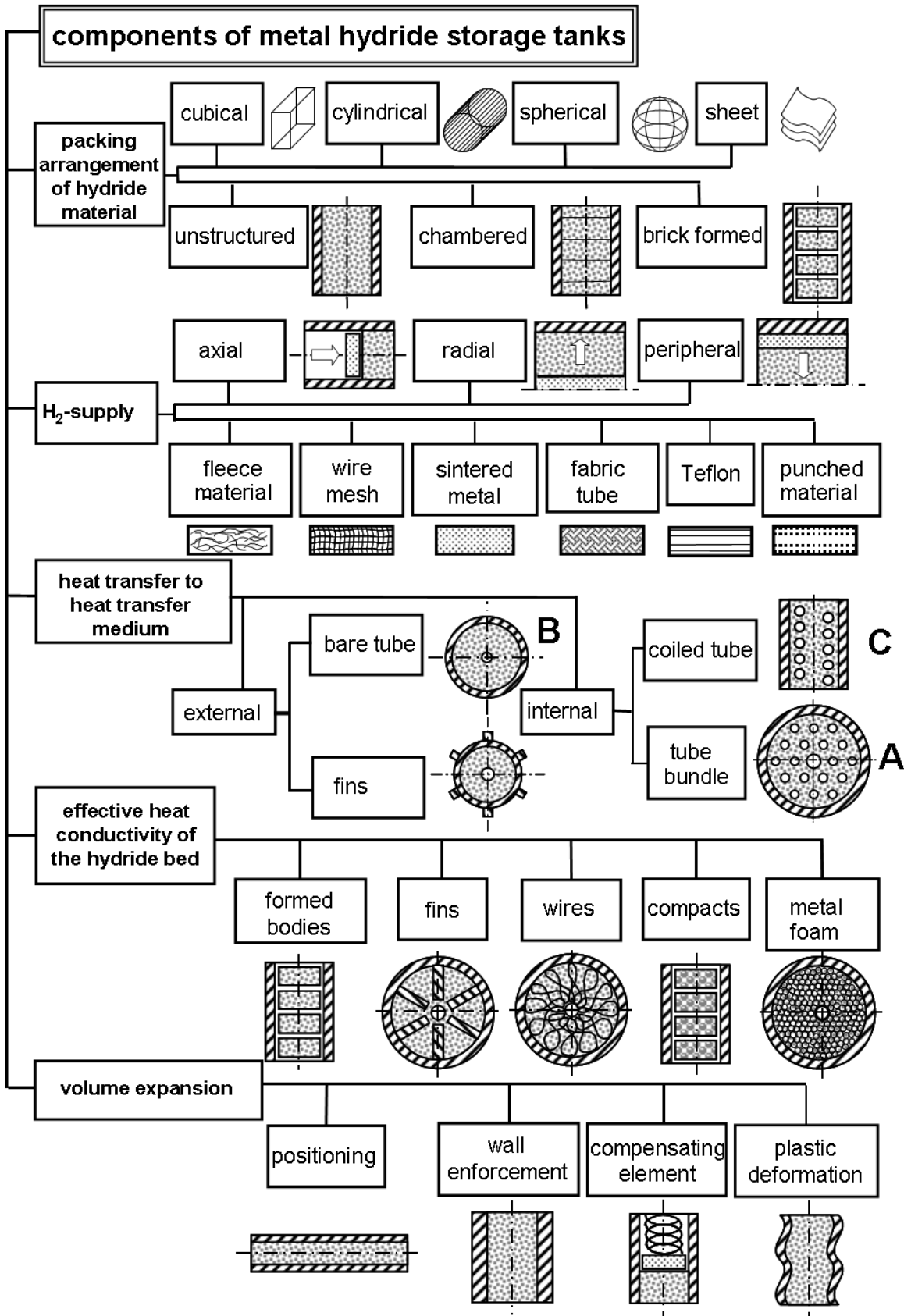**Figures**

Figure 1: Working principle of a tubular reactor
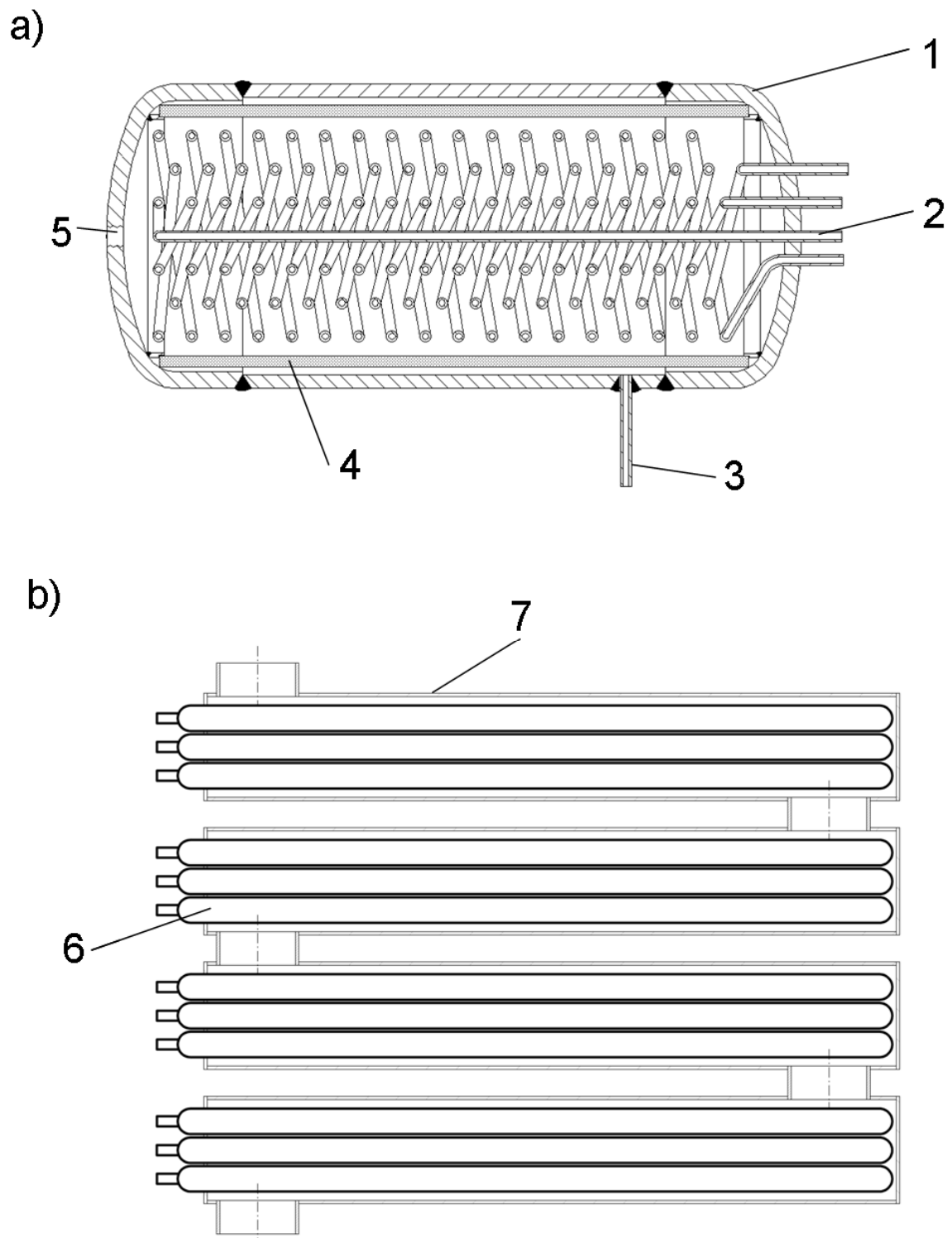
components of metal hydride storage tanks

packing arrangement of hydride material

cubical	cylindrical	spherical	sheet

unstructured	chambered	brick formed

H₂-supply

axial	radial	peripheral

fleece material	wire mesh	sintered metal	fabric tube	Teflon	punched material

heat transfer to heat transfer medium

external — bare tube | fins

B

internal — coiled tube | tube bundle

C

A

effective heat conductivity of the hydride bed

formed bodies	fins	wires	compacts	metal foam

volume expansion

positioning	wall enforcement	compensating element	plastic deformation

Figure 2: Design principles of metal hydride storage tanks

a)

b)

Figure 3: Favored design concepts. a) Elaborated version of large hydride vessel: (1) shell, (2) coiled tube for heat transfer fluid, (3) hydrogen nozzle, (4) peripheral hydrogen supply, (5) opening for filling in active material. b) Modular concept: (6) tubular reactor element, (7) heat transfer fluid shell.
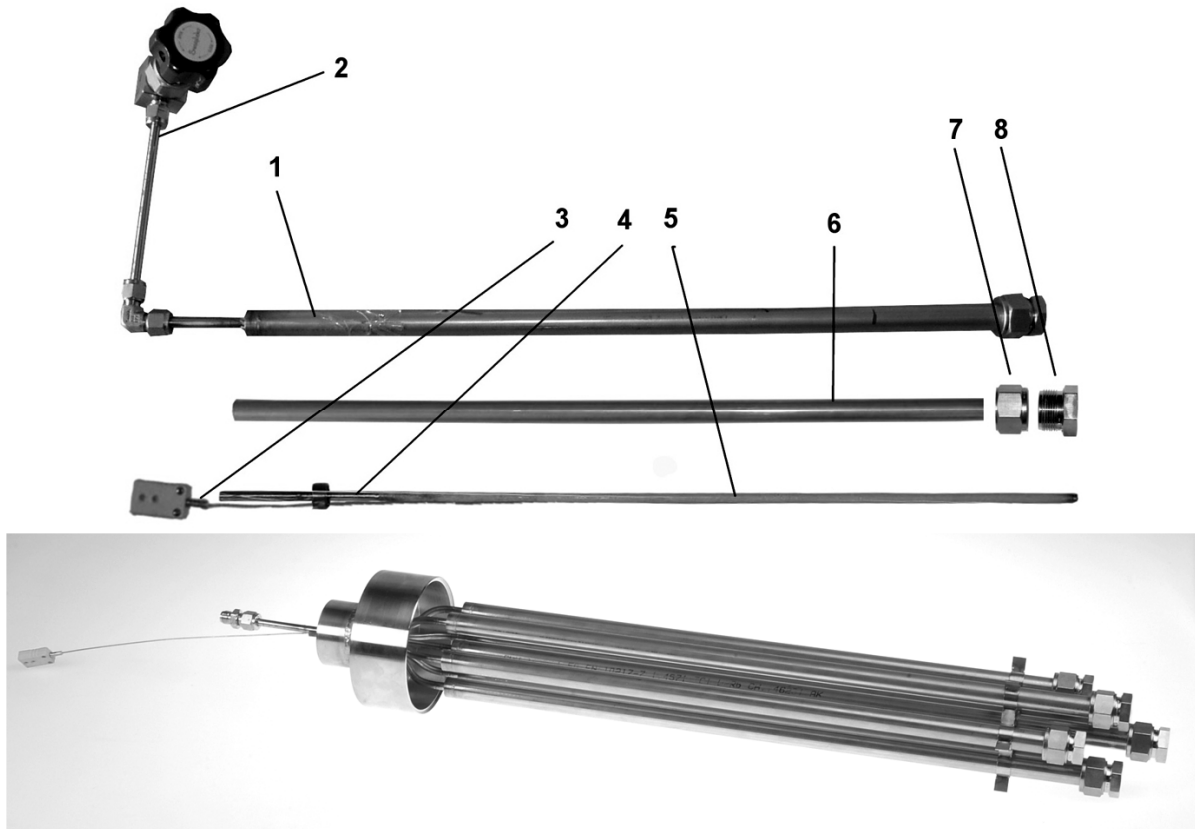
Figure 4: Laboratory-scale tubular reactor and arrangement to a tube bundle. (1) tubular reactor, (2) hydrogen valve, (3) thermocouple, (4) gastight hydrogen supply tube, (5) porous sintered metal tube, (6) reactor shell tube, (7) closure nut, (8) closure plug
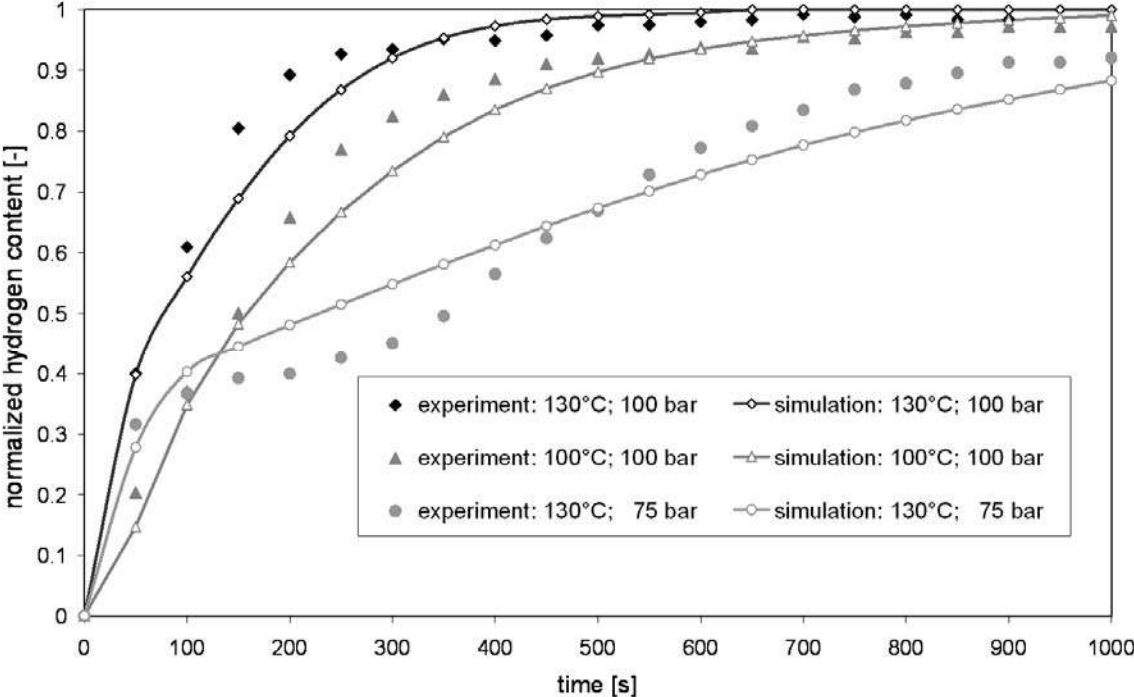
Figure 5: Results of preliminary experiments validating the model
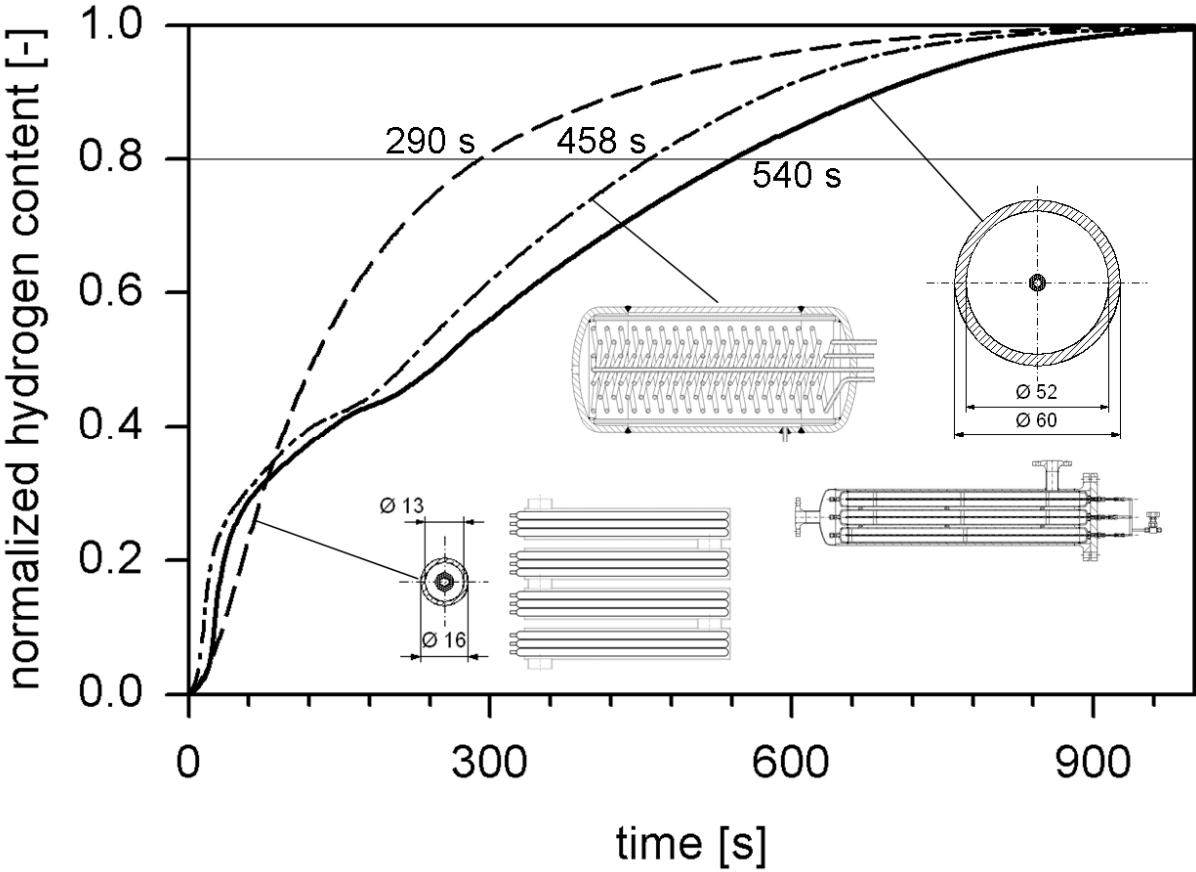
Figure 6: Simulation results
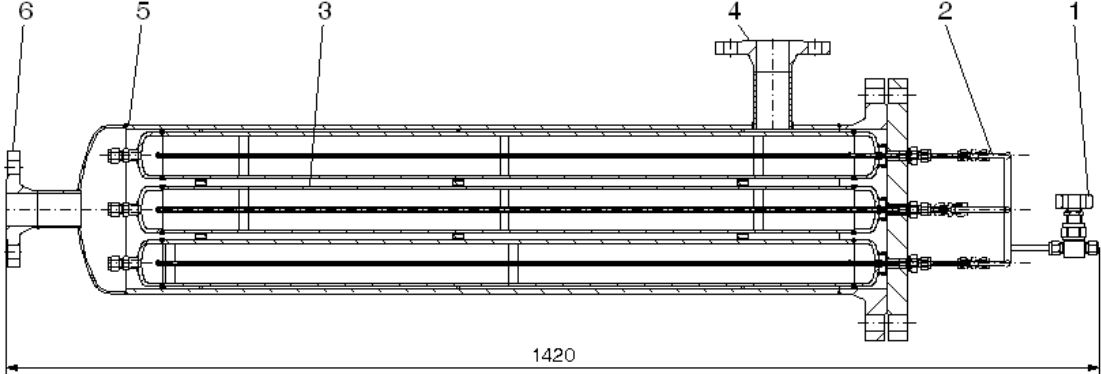
Figure 7: Prototype design: (1) hydrogen valve, (2) hydrogen supply spiral, (3) reactor element, (4) inlet nozzle of the heat transfer fluid, (5) shell, (6) outlet nozzle
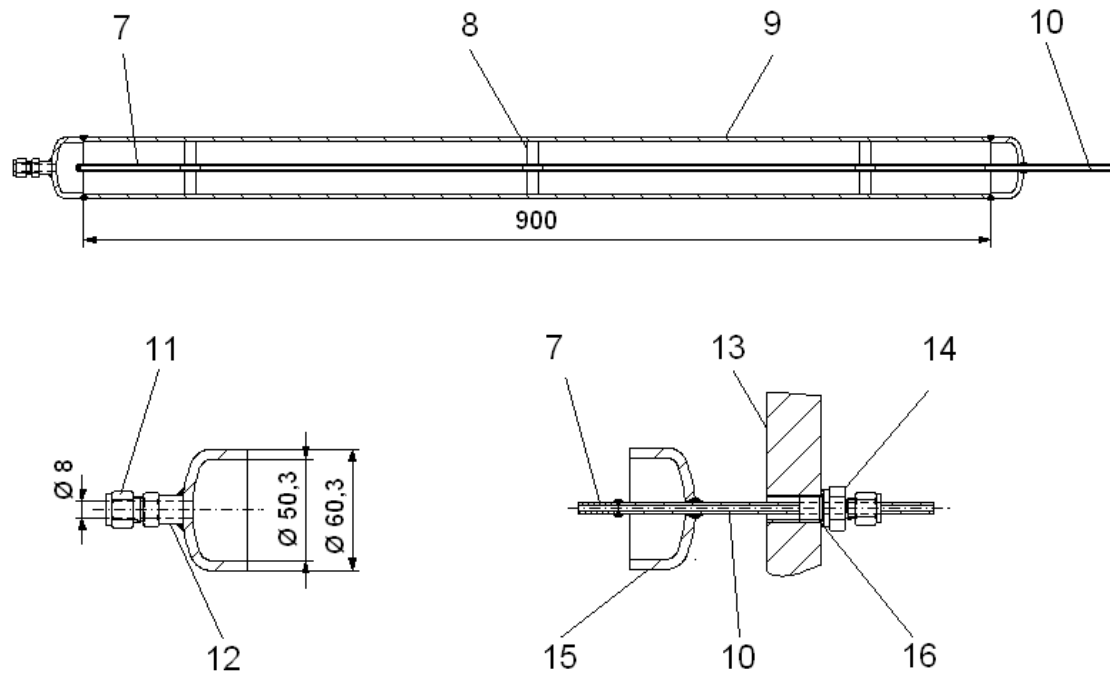
Figure 8: Details of reactor element: (7) porous sintered metal tube, (8) support of sintered metal tube, (9) reactor element shell, (10) gastight hydrogen supply tube, (11) closure plug, (12) male connector (bored through, 8 mm for filling of active material under glove box conditions), (13) flange, (14) male connector (bored through), (15) torispherical head, (16) copper gasket
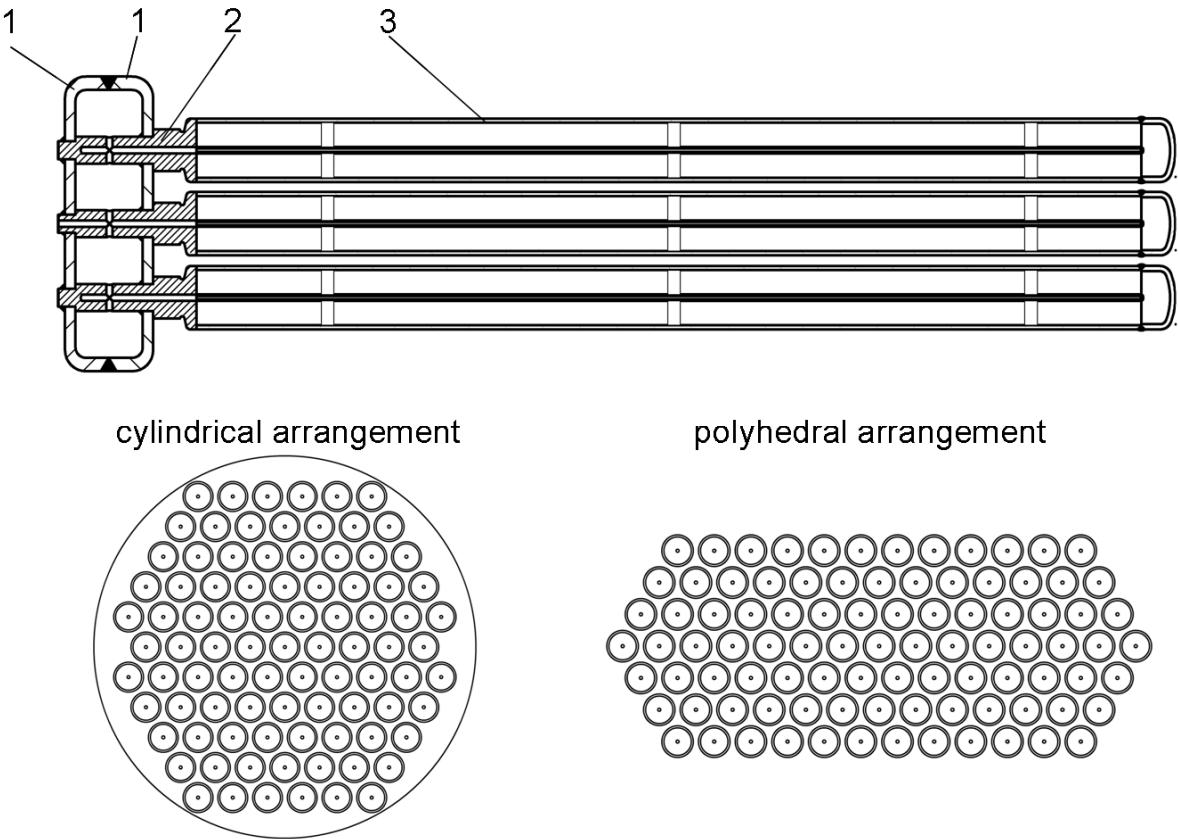
Figure 9: Manufactured prototype

Figure 10: Scale-up with principle of an advanced hydrogen manifold. (1) flanged flat end, (2) stay bolt as hydrogen supply, (3) reactor element

26

List of Tables

Short Text – Table of Contents of the Journal

The systematic design of the prototype of a solid storage tank for hydrogen based on sodium alanate is presented. At first the developed model-based design tool is validated by experiments with a small-scale tubular reactor. After analysis of the simulation results the final design of the prototype is illustrated. Already with respect to the design of even larger storage tanks a modular concept is chosen enabling scale-up to fuel cell vehicle storage tanks containing 5 kg of hydrogen.